

Catalysis Science & Technology

Accepted Manuscript



This is an *Accepted Manuscript*, which has been through the Royal Society of Chemistry peer review process and has been accepted for publication.

Accepted Manuscripts are published online shortly after acceptance, before technical editing, formatting and proof reading. Using this free service, authors can make their results available to the community, in citable form, before we publish the edited article. We will replace this *Accepted Manuscript* with the edited and formatted *Advance Article* as soon as it is available.

You can find more information about *Accepted Manuscripts* in the [Information for Authors](#).

Please note that technical editing may introduce minor changes to the text and/or graphics, which may alter content. The journal's standard [Terms & Conditions](#) and the [Ethical guidelines](#) still apply. In no event shall the Royal Society of Chemistry be held responsible for any errors or omissions in this *Accepted Manuscript* or any consequences arising from the use of any information it contains.



Catalysis Science and Technology

ARTICLE

Graphene decorated with Fe nanoclusters for improving the hydrogen sorption kinetics of MgH₂ – Experimental and theoretical evidence

Received 06th July 2015,
Revised 29th July 2015
Accepted 00th January 20xx

M. Sterlin Leo Hudson^{a,†}, Keisuke Takahashi^{b,†}, A. Ramesh^a, Seema Awasthi^c, Ashish Kumar Ghosh^d and Onkar Nath Srivastava^e

DOI: 10.1039/x0xx00000x

www.rsc.org/

Graphene decorated with Fe clusters is proposed to be a possible alternative catalyst for the hydrogenation and dehydrogenation reactions of MgH₂. In particular, graphene decorated with Fe clusters is effective for both the hydrogenation and dehydrogenation processes of MgH₂. The change in enthalpy and entropy values of hydrogen absorption determined for MgH₂ with 5wt.% graphene decorated Fe cluster are -50.4 ± 2.9 kJmol⁻¹ H₂ and 99.8 ± 5.2 JK⁻¹mol⁻¹ H₂, respectively. This is significantly lower than the well-established metal catalysts and the nano-interfacial confined MgH₂. Moreover, the graphene decorated with Fe clusters helps the fast rehydrogenation kinetics of MgH₂, which reabsorbed 90% of the total reabsorption capacity in less than 4 minutes at 300°C and 20 atm. In addition, TEM analysis reveals that MgH₂ particles are covered by graphene with Fe clusters, resulting in the reduction of grain growth. Density functional theory shows that defects of graphene act as the active sites for dehydrogenation of MgH₂ while Fe clusters reduce the adsorption of dissociated H atoms, resulting in low temperature dehydrogenation. Thus, graphene decorated with metal clusters could open up a new way of designing a new type of catalysts which could replace transition metal catalysts.

Introduction

Functionalized graphene has quickly caught much attention due to its unexpected properties in the field of catalysis.¹ Graphene oxide is a successful modification of graphene where graphene oxide shows high catalytic activity during the oxidation process.^{2,3} In the same fashion, metal-cluster decorated graphene happens to have unexpected catalytic effects towards various systems.⁴⁻⁶ In particular, graphene decorated with iron clusters is experimentally and theoretically found to store hydrogen.^{7,8} During the hydrogen absorption process over graphene with iron clusters, calculations also revealed that H₂ dissociation occurs over iron clusters, which is considered to cause spillover towards graphene.⁷ Such phenomena can be a key reaction for the hydrogenation process as the H₂ dissociation is generally a first step reaction for hydrogenation reaction. Here, magnesium hydride (MgH₂) is chosen to evaluate the catalytic effect of graphene with Fe nano clusters. Magnesium hydride is a potential hydrogen storage material containing 7.6 wt.% H₂ (theoretical capacity). However, an

effective catalyst is required to overcome the high thermodynamic stability and slow hydrogenation reaction kinetics of MgH₂. Magnesium hydride is the prototype hydrogenation reaction which requires Mg, H₂ and MgH₂ dissociation. In order to improve the kinetics of the hydrogenation and dehydrogenation of magnesium hydride, tremendous amount of catalysts have been extensively investigated.⁹⁻¹⁴ However, seeking better catalysts for accelerating kinetics, hydrogenation, and dehydrogenation of MgH₂ are still problematic issues for further practical applications. Metal decorated graphene catalysts could be proposed to be potential catalysts for hydrogenation reaction for such systems. The catalytic effect of graphene decorated with iron clusters is experimentally and theoretically investigated.

In particular, MgH₂ is used as a prototype reaction in order to evaluate the catalytic effect towards hydrogenation and dehydrogenation process. Hydrogen absorption and desorption of MgH₂ with graphene decorated with iron clusters are experimentally tested. Transmission electron microscope imaging is used to observe the microstructure of graphene, iron, and MgH₂. Density functional theory is implemented in order to reveal the physical and chemical origin of the reaction mechanism. Although the study takes place for iron decorated graphene and MgH₂, the catalytic effect and mechanism of graphene with metal systems should be generalized and help further develop metal decorated graphene catalysts.

^a Department of Physics, Central University of Tamil Nadu, Thiruvavur – 610101, India.

^b Graduate School of Engineering, Hokkaido University, Sapporo 060-8278, Japan.

^c School of Physics, Hyderabad Central University, Hyderabad-500046, India.

^d Central Institute of Mining and Fuel Research, Dhanbad-826001, India.

^e Department of Physics, Banaras Hindu University, Varanasi-221005, India.

† Corresponding Author, Email: msterlinleo@cutn.ac.in (MSLH), keisuke.takahashi@eng.hokudai.ac.jp (KT), Phone: +91-9486-860214 (MSLH), Phone: 81-11-706-6772 (KT)

Electronic Supplementary Information (ESI) available: [details of any supplementary information available should be included here]. See DOI: 10.1039/x0xx00000x

ARTICLE

Catalysis Science and Technology

Experimental

MgH₂ powder of purity 98% and Fe nanopowder (APS 10-30 nm) of purity 99.9% were purchased from Alfa Aesar. Graphene decorated with Fe nanoclusters (G-Fe) were synthesized in an electric arcing chamber using graphite electrodes. To ablate the material, an electric arc was generated using a DC source of 100A and 25V between a pure graphite rod (cathode) placed opposite to a grounded anode rod made of graphite impregnated with Fe nanopowder in an arcing chamber filled with Ar (99.999% purity) partial pressure of ~300 torr. After 8-10 min of the arcing process, the flake like carbon material was found deposited around the walls of the arcing chamber which was later confirmed as G-Fe. The MgH₂ powder was ball-milled together with 5 wt.% G-Fe under 5 atm hydrogen pressure in a custom fabricated stainless steel vial of volume 250 cm³ (capable of retaining up to 60 atm pressure) using a Retsch PM 400 planetary ball-miller at an operating speed of 150 rpm for a period of 60 minutes (6 ×10 minutes ball-milling with 15 minutes interval in-between). The ball to powder ratio was kept at 30:1, where the weight of the sample was around 2.5 grams. Ball-milling under hydrogen atmosphere prevents MgO formation¹³. For comparative analysis, MgH₂ (without G-Fe) was ball-milled under identical experimental conditions for 5 hours (30×10 minutes ball-milling with 15 minutes interval in-between). Handling of the samples was done in mBraun MB10 compact Ar filled glove box (H₂O and O₂ levels < 1 ppm).

Dehydrogenation and reabsorption kinetics of the samples were analyzed through temperature programmed desorption (TPD) and pressure composition isotherm (PCI) using an auto-mated four channel volumetric Sieverts type apparatus supplied by Advanced Materials Corporation. TPD analysis of sample was done at the initial pressure of 10⁻³ torr under dynamic heating condition with an accuracy of ±0.2°C. Rehydrogenation kinetics were measured at different temperatures by charging the dehydrogenated MgH₂ samples with 20 atm hydrogen pressure. Thermal analyses of samples were conducted using a differential scanning calorimeter (DSC 8000, PerkinElmer). The samples were heated from room temperature to about 500°C with a set heating rate under flowing argon of 20ml/min.

Structural characterizations of the samples were investigated by X-ray diffraction using PANalytical X'Pert PRO diffractometer with a Cu K_α beam ($\lambda = 1.5415 \text{ \AA}$) operated at 40 kV and 40 mA. The samples were loaded in airtight sample holders sealed by a fine layer of parafilm (Pechiney plastic packing) to prevent the sample from oxygen and moisture contamination.¹⁴ Microstructures of the samples were analyzed through bright field imaging and selected-area electron diffraction (SAED) using a FEI Tecnai 20G² transmission electron microscope (TEM) operated at 200 keV.

Results and discussion

TPD of MgH₂ samples was performed from room temperature (25°C) to 450°C under dynamical heating condition at the heating rate 2°C/min. A comparative TPD profiles of MgH₂

pristine, 5 hours ball-milled MgH₂ (un-catalyzed) and MgH₂+5wt.% G-Fe is shown in Fig. 1(a) & 1(b).

It has been observed from the TPD profiles that the dehydrogenation temperature of MgH₂+5wt.% G-Fe is significantly lower than pristine and ball-milled MgH₂. The peak temperature of MgH₂+5wt.% G-Fe is 281.7°C, whereas that of 5 hours ball-milled MgH₂ shows peak temperature at 322.3°C. This suggest that graphene together with Fe nanoclusters exhibit superior catalytic effect in improving the dehydrogenation behaviour of MgH₂.

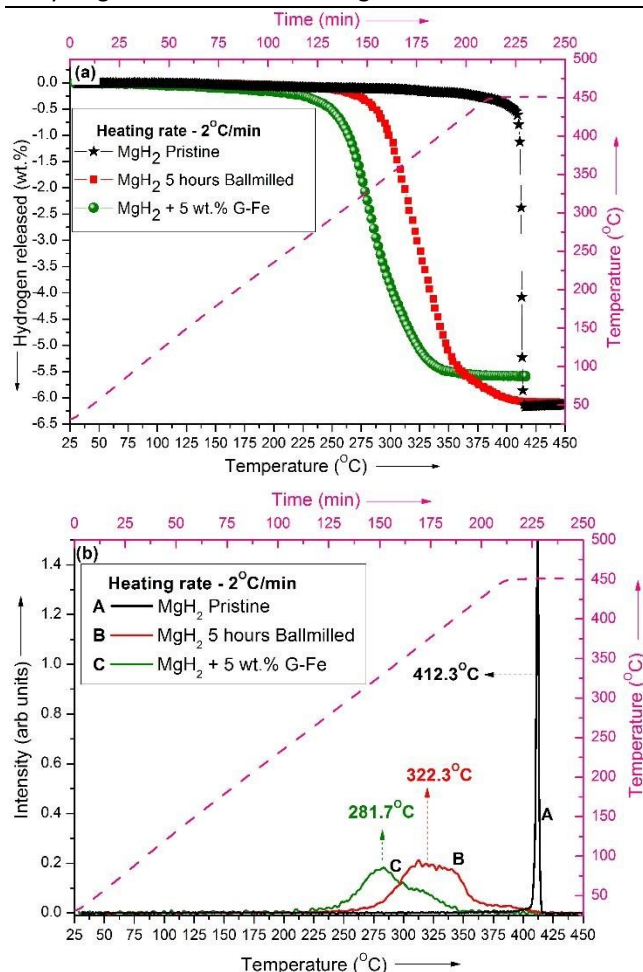


Fig. 1. Comparative TPD profiles of MgH₂ (a) hydrogen release capacity and (b) peak temperature

Fig. 2(a) & 2(b) presents the DSC curves of 5 hours ball-milled (un-catalyzed) MgH₂ and MgH₂ + 5 wt.% G-Fe, respectively, determined at different heating rates (2, 5, 10 and 15°C/min). The apparent activation energy (E_a) of ball-milled MgH₂ and MgH₂ + 5 wt.% G-Fe was determined using the Kissinger method.¹⁵

The peak desorption temperature (TPD) determined from the DSC curves and the corresponding heating rates (β) are the two parameters required for finding E_a using the Kissinger equation given below.

$$\ln(\beta/T_p^2) = (-E_a/RT_p) + \ln(k_0) \quad (1)$$

Where, k_0 is a constant. A plot of $\ln(\beta/T_p^2)$ vs $1/T_p$ has a negative slope. Here, we have used 2, 5, 10 and 15°C/min DSC heating rates for calculating activation energy of the samples. Corresponding $\ln(\beta/T_p^2)$ vs $1/T_p$ plot of MgH_2 ball-milled and $\text{MgH}_2 + 5\text{wt.}\%$ G-Fe is shown in Fig. 2(c).

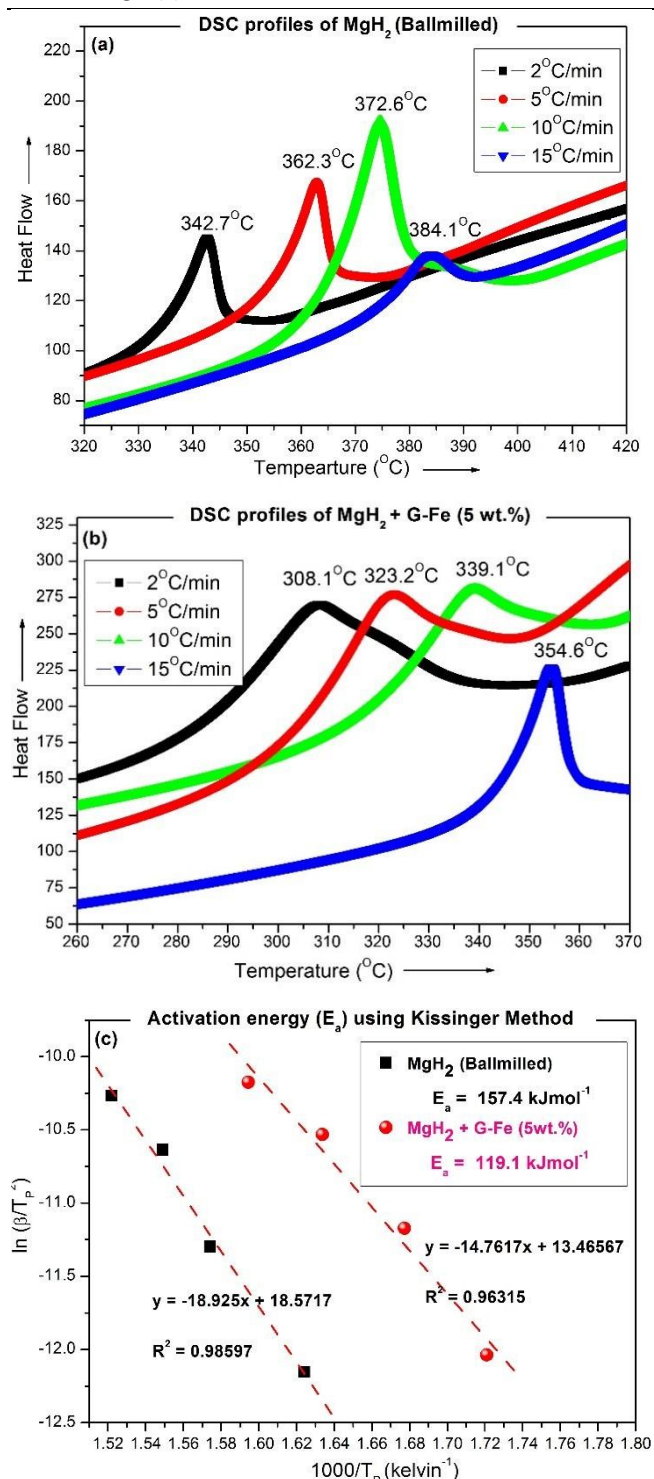


Fig. 2. DSC curves measured at different heating rates (a) MgH_2 Ball-milled, (b) $\text{MgH}_2 + 5\text{wt.}\%$ G-Fe and (c) $\ln(\beta/T_p^2)$ vs $1/T_p$ plot.

The desorption activation energy of ball-milled MgH_2 (w/o additive) and 5 wt.% G-Fe admixed MgH_2 determined from

the DSC curves using Kissinger method are 157.4 and 119.1 kJmol^{-1} . For pristine MgH_2 , it is $\sim 187\text{ kJmol}^{-1}$.^{16,17} Table. 1 gives the summary of the calculated apparent activation energy of MgH_2 determined from DSC curves using Kissinger equation.

Table 1. Summary of desorption activation energy determined for MgH_2 using Kissinger method

	Pristine MgH_2	5 hours Ball-milled MgH_2	$\text{MgH}_2 + \text{G-Fe}$ (5wt.%)
Activation Energy (kJmol^{-1})	~ 187 ^{16,17}	157.4	119.1

It should be noted that 1 hour ball-milled $\text{MgH}_2 + 5\text{ wt.}\%$ graphene nanosheets (without metal decoration) shows the peak desorption temperature at 358°C for the DSC heating rate of 5°C/min.¹⁸ Whereas, in the present case, for 1 hour ball-milled $\text{MgH}_2 + 5\text{ wt.}\%$ G-Fe shows the peak desorption temperature at 323°C for the DSC heating rate of 5°C/min (refer Fig. 2(b)). Thus the presence of Fe nanoclusters on graphene greatly lowers the dissociation temperature of MgH_2 .

Fig. 3 presents the isothermal reabsorption kinetic curves of dehydrogenated $\text{MgH}_2 + 5\text{wt.}\%$ G-Fe determined at different temperatures with 20 atm hydrogen pressure. It has been observed that the dehydrogenated $\text{MgH}_2 + \text{G-Fe}$ sample shows fast absorption kinetics. The sample absorbed more than 5 wt.% hydrogen in less than 4 minutes at 300°C and 20 atm. Whereas, that of ball-milled (un-catalyzed) dehydrogenated MgH_2 sample took nearly 20 min to absorb 5 wt.% hydrogen at 300°C and 20 atm. This reveals that the G-Fe exhibit superior catalytic effect on MgH_2 both for hydrogen release and uptake.

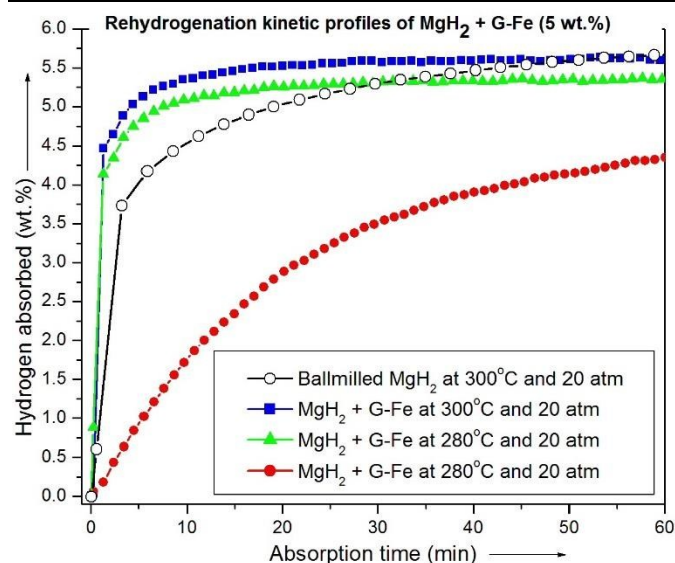


Fig. 3. Reabsorption kinetic curves of dehydrogenated $\text{MgH}_2 + \text{G-Fe}$

Fig. 4(a) & 4(b) represents the PCI isotherms and Vant Hoff plot of $\text{MgH}_2 + \text{G-Fe}$, respectively. From the Vant Hoff plot (Fig. 4(b)), the formation enthalpy and entropy values of MgH_2 with 5 wt.% G-Fe were derived. The change in enthalpy and entropy values are $-50.4 \pm 2.9\text{ kJmol}^{-1}\text{ H}_2$ and $99.8 \pm 5.2\text{ JK}^{-1}\text{mol}^{-1}\text{ H}_2$, respectively for the formation of MgH_2 . It should be mentioned that the change in formation enthalpy and entropy value for as-received bulk MgH_2 is -

ARTICLE

Catalysis Science and Technology

74.06 ± 0.42 kJmol⁻¹ H₂ and 133.4 ± 0.7 JK⁻¹mol⁻¹ H₂, respectively.¹⁹ However, change in formation enthalpy and entropy of MgH₂ was reported for element coated Mg. For Fe coated Mg, the formation enthalpy and entropy of MgH₂ was -59.9 ± 1.9 kJmol⁻¹ H₂ and 112.3 ± 3.1 JK⁻¹mol⁻¹ H₂, respectively.²⁰

Zhao-Karger *et al.*²¹ reported that MgH₂ nanoparticles (< 3 nm) confined in activated carbon fiber scaffold system exhibits a reduced enthalpy and entropy values of -63.8 kJmol⁻¹ H₂ and 117.2 JK⁻¹mol⁻¹H₂, respectively. Jia *et al.*²² observed that MgH₂ nanoparticles into (1-2 nm) and onto (5-6 nm) ordered mesoporous carbon, CMK-3 exhibits a reduced enthalpy and entropy of -55.4 kJmol⁻¹ H₂ and 105.7 JK⁻¹mol⁻¹H₂, respectively. Recently, reduced enthalpy and entropy values of -45 ± 3 kJmol⁻¹ H₂ and 84 ± 5 JK⁻¹mol⁻¹ H₂, respectively were observed for MgH₂-Ti nanocomposites produced by spark discharge.¹²

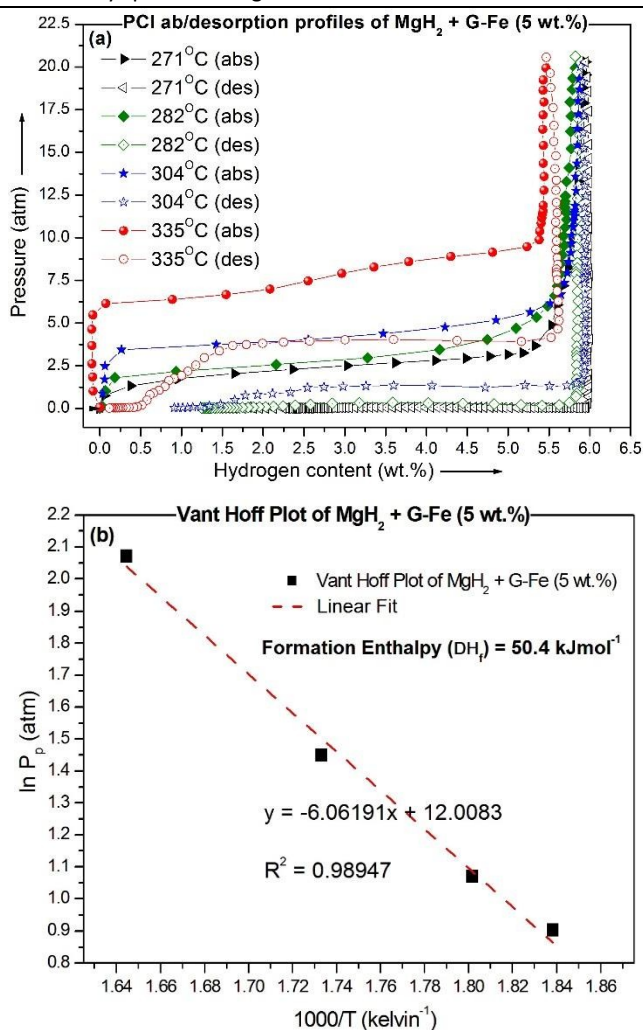


Fig. 4. (a) PCI desorption and absorption curves of MgH₂ + G-Fe determined at different temperatures (b) Vant Hoff plot of MgH₂ + G-Fe

It is known that the thermodynamic properties of the Mg-to-MgH₂ hydrogenation reaction may change dramatically at the nanoscale due to its modified structure at the nano dimension and the dominant contribution of the surface (or interface) structure and local bond lengths at the smallest sizes.¹² In accordance with the previous reports, it is known that Fe nanoparticles²³ and

graphene^{18,24} are very good catalyst for MgH₂ system. Therefore, in the present investigation, the observation of low reaction enthalpy and entropy values for the hydrogenation reaction of Mg is due to the nanosize and intermixed character of the disordered graphene and Fe nanoparticles. The presence of Fe nanoparticles and graphene is expected to have a synergetic effect in improving the dehydrogenation behavior and in enhancing the hydrogenation of Mg to MgH₂ through spillover effect.^{25,26}

Fig. 5(a) shows the XRD patterns of as prepared MgH₂+5wt.% G-Fe, Fig. 5(b) presents the dehydrogenated XRD pattern after five rehydrogeation cycles of MgH₂+G-Fe (5 wt.%) and Fig. 5(c) shows its XRD pattern after sixth rehydrogenation cycles.

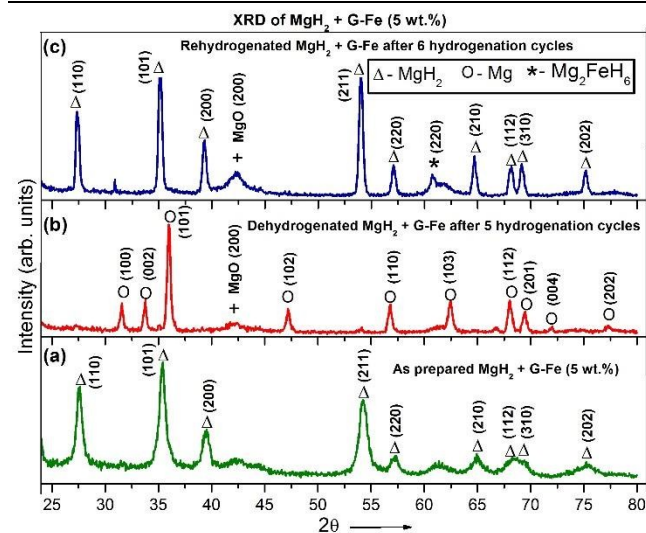


Fig. 5. Powder X-ray diffraction pattern of MgH₂ + G-Fe (a) as prepared (b) Dehydrogenated after five hydrogenation cycles and (c) Sixth hydrogenation cycles.

It was found that along with main MgH₂ phase, MgO phase is detected. It was noticed that after sixth dehydrogenation and rehydrogenation cycles, the diffraction peak intensity increases, suggesting the grain growth of MgH₂. Assuming MgH₂ particles are spherical, the size of grains were calculated from XRD peaks using the Scherrer equation.²⁷ This suggest that the average grain size of as-prepared MgH₂+G-Fe (Fig. 5(a)) is 19 nm and after sixth cycles (Fig. 5(c)), the grain size of MgH₂ increases to 34.8 nm. Liu *et al.*²⁴ observed that after six hydrogenation cycles, the grain size of pure-MgH₂ (w/o additives) was increased three times (from 10.8 nm before cycling to 32 nm after cycles).

The nucleation and growth of Mg₂FeH₆ phase was observed in the cycled MgH₂+G-Fe sample, due to the reaction between elemental Mg and Fe during hydrogenation process, suggesting that the Fe particles are not free during hydrogenation. However, during dehydrogenation, the Mg₂FeH₆ completely transformed into elemental phases of Mg and Fe, helpful for the initial stage of the rehydrogenation process.²⁸

Microstructural analysis of the sample was carried out using TEM. Fig. 6 presents the TEM microstructures of as-synthesized graphene sheets decorated with Fe nanoclusters (Fig. 6(a)), MgH₂ ball-milled for 5 hours (Fig. 6(b)), MgH₂ + 5wt.% G-Fe (Fig. 6(c)) and after five dehydrogenation/ rehydrogenation cycles (Fig. 6(d)).

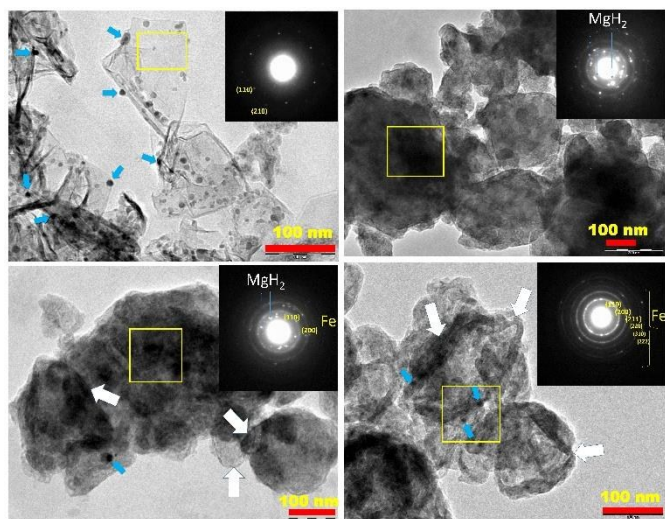


Fig. 6. TEM microstructure of (a) as-synthesized G-Fe, (b) MgH_2 ball-milled for 5 hours, (c) as-prepared MgH_2 +G-Fe and (d) MgH_2 +G-Fe after six dehydrogenation and rehydrogenation cycles. Inset shows the corresponding SAED pattern.

It was found from the TEM micrograph (Fig. 6(a)) that the Fe nanoparticles (indicated by blue arrow) in G-Fe were found to get decorated throughout the graphene surface. The size of Fe nanoparticles are in the range of 5 to 15 nm. The hexagonal pattern observed in SAED (inset of Fig. 6(a)) confirms the synthesized sample is graphene. EDAX spectral analysis confirms the composition of Fe nanoparticles in graphene is 2 wt.%. Supplementary figures, Fig. S1 and Fig. S2 shows the representative Raman and energy dispersive X-ray (EDX) spectrum of as prepared G-Fe. The distribution of graphene sheets (shown by white arrow) can be readily distinguished in the as-prepared and cycled MgH_2 +G-Fe samples (Fig. 6(c) & 6(d)). The corresponding SAED patterns (insets in Fig. 6(c) & 6(d)) shows the fine grain distribution of the samples. The ring patterns arise in the SAED patterns due to the presence of Fe nanoparticles and the bright patterns are from MgH_2 particles. It has been observed from the TEM micrograph of cycled sample that the graphene is intercalated between MgH_2 particles, possibly reducing the agglomeration of MgH_2 particles during cycling. In accordance with the earlier study by other researchers, it has been observed that the presence of graphene reduces the grain growth of MgH_2 , suggesting graphene is a very good crystal growth inhibitor during dehydrogenation/ rehydrogenation cycles of MgH_2 .^{25,26}

In order to further understand the synergetic effect of Fe nanoclusters and graphene, we have done *ab-initio* studies which are described below.

Computational Method

Grid based Projector-Augmented Wave method (GPAW) is implemented within the density functional theory.²⁹ The grid spacing is set to 0.20 Å with 0.00 eV of smearing. The Γ point is implemented for the sampling of the Brillouin-zone. Exchange-correlation of Perdew-Burke-Ernzerhof (PBE) with spin polarization calculations are applied for all calculations.³⁰ Charge transfer analysis is performed using the Bader charge analysis.^{31,32}

Adsorption energies of MgH_2 cluster and one H atom are calculated by the equation (2)

$$E_{ad} = E_{[Surface+Adsorbate]} - E_{[Surface]} - E_{[Adsorbate]} \quad (2)$$

The reaction between Fe decorated graphene and MgH_2 takes place by using the mechanical ball milling process in the experiment. In general, the ball milling process destroys the structure of material. Hence, atomic clusters are implemented in order to consider the complicated unusual structures. MgH_2 cluster is used in order to understand the fundamental dehydrogenation properties over the Fe decorated catalysts as MgH_2 clusters have been shown to be an effective model to understand the hydrogenation and dehydrogenation properties of MgH_2 systems.¹⁰ In addition, graphene within non periodic boundary conditions is considered. In particular, asymmetry graphene consisting of 32 carbon atoms shown in Fig. 7(a) are constructed within non periodic boundary conditions.

Computational Results

MgH_2 cluster is adsorbed in non-defected graphene with/without Fe atom, single defected graphene, Fe doped graphene and large graphene with/without Fe atom. The adsorption of energies of MgH_2 cluster and H atom over each graphene model are collected in Table 2. The structural model is shown in Fig. 7 (a-f). The different sizes of defect and adsorption of Fe monomers are considered based on the graphene in Fig. 7(a).

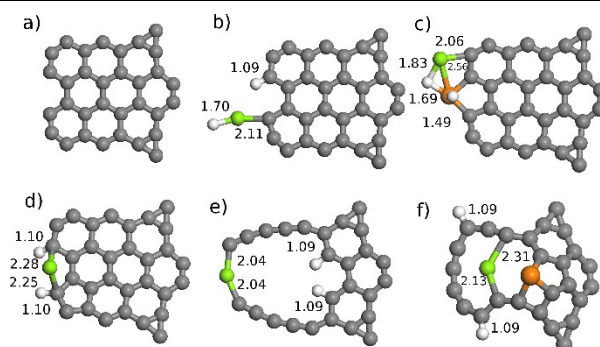


Fig. 7 (a) Asymmetry graphene, (b) MgH_2 cluster on symmetry graphene, (c) MgH_2 cluster on Fe doped asymmetry graphene, (d) MgH_2 on single defected graphene, (e) MgH_2 cluster on large defected graphene, (f) MgH_2 cluster on large defected graphene with Fe. Inter atomic distance of H-C, Mg-C, Mg-H, Mg-Fe, Fe-H are shown in Å. Atomic color codes: Mg, Green; H, White; C, Gray; Fe, Orange.

MgH_2 cluster is adsorbed on the edge of non-defected graphene where one of the H atoms is dissociated and adsorbed on C atom. The adsorption energy of MgH_2 cluster and the H atom on non-defected graphene is calculated to be -4.21eV and -0.55 eV, respectively. Upon the introduction of Fe atom on non-defected graphene, both H atoms are fully dissociated from MgH_2 clusters as shown in Fig. 7(c). In particular, it is interesting that the adsorption energy of the MgH_2 cluster and H atom dramatically decreased and has -1.36 eV and 0.06 eV compared to one without Fe. Thus, a dramatic decrease of H adsorption energy is predicted to allow low temperature dehydrogenation. Single C defect is created at the edge

of graphene shown in Fig. 7(d). Both H atoms are dissociated over the single C defected graphene. It is interesting that the adsorption energy of MgH₂ cluster on single defect graphene is calculated to be -5.38 eV as single defect enhance -1.17eV of the MgH₂ cluster adsorption energy compared to MgH₂ cluster on non-defected graphene. Furthermore, H adsorption energy is calculated to be -0.83 eV where H atoms are adsorbed at the edge of graphene shown in Fig. 7(d). However, a decrease of H adsorption energy is not observed in the single defect case compared to the case of Fe decorated graphene.

A large defect is created in graphene in order to completely break the structure of graphene where six carbon atoms are taken from graphene consisting of 32 C atoms. The structure of graphene is greatly deformed. MgH₂ cluster adsorption on the large defected graphene particularly shows a high adsorption energy of -7.89 eV where both H atoms are dissociated from MgH₂ cluster as shown in Fig. 7(e). H adsorption energy is calculated to be -2.08 eV. This also confirms that the edge of the defected graphene is reactive against MgH₂ cluster. However, high H adsorption energy could require higher temperatures for further dehydrogenation processes. A Fe atom is then adsorbed on the large defected graphene shown in Fig. 7(f). The adsorption energy of MgH₂ cluster and H atom over the large defected graphene with Fe is dramatically decreased to -2.84 eV and -0.53 eV, respectively where full dehydrogenation of MgH₂ cluster is also observed. Thus, one can suggest that the introduction of Fe atom decreases the dehydrogenation temperature of MgH₂ cluster over defected graphene.

Bader charge analysis is performed for the large defect graphene with/without Fe in order to reveal the physical origin of the effect of Fe. Bader analysis indicates that Fe atom is positively charged by 0.8 electrons. This indicates that electrons from Fe atoms are transferred to C atoms near Fe atoms. One could suggest that Fe atoms fill and stabilize the defect of graphene. As a result, graphene is less active. On the other hand, electrons in the d-orbital of Fe atoms could enhance the dehydrogenation of MgH₂ cluster. Thus, the catalytic activities of defected graphene could be controlled by Fe.

Table 2. MgH₂ adsorption energy E(MgH₂) and hydrogen desorption energy E(H) in eV over various graphene condition

	EMgH ₂	EH
Non-defected graphene	-4.21	-0.55
Non-defected graphene + Fe	-1.36	-0.06
Single defected graphene	-5.38	-0.83
Large defected graphene	-7.89	-2.08
Large defected graphene + Fe	-2.48	-0.53

Conclusions

Graphene decorated with Fe clusters is experimentally and theoretically proven to be a possible low cost and alternative catalyst towards the hydrogenation reaction compared to transition metal catalysts. Experiment shows that graphene decorated Fe clusters decrease the dehydrogenation temperature of MgH₂ from 322.3°C to 281.7°C where activation energies are experimentally measured to be 119.1 kJmol⁻¹. Furthermore, the rehydrogenation of MgH₂ with

graphene decorated Fe clusters is dramatically improved where it takes only 4 minutes to absorb 5 wt% of hydrogen at 300°C and 20 atm. After the six rehydrogenation cycles, the grain size of MgH₂ increased only 15 nm, showing a low order grain growth during cycling. This is advantageous for MgH₂ in withstanding cycling stability, suitable for hydrogen storage applications. The TEM analysis confirms the low order grain growth of MgH₂ and shows that the graphene decorated Fe cluster behaves like a shell while MgH₂ is its core. Density functional theory calculations reveal that the location of the active site- the defect in graphene and the presence of iron clusters at the defect site of graphene are the key factors for the dehydrogenation of MgH₂, as the Fe clusters reduce the adsorption of dissociated H atoms, thereby resulting in low-temperature hydrogen release. This suggests that other transition metals could also be effective if charge transfers from the transition metal to graphene are involved. Thus, graphene decorated with Fe clusters could be a potential alternative for transition metal catalysts for hydrogenation reaction and have a possibility to seek further graphene decorated with other metal clusters.

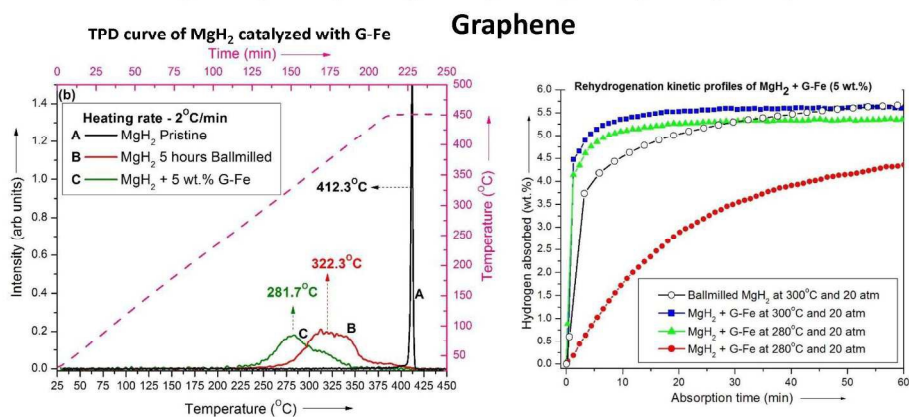
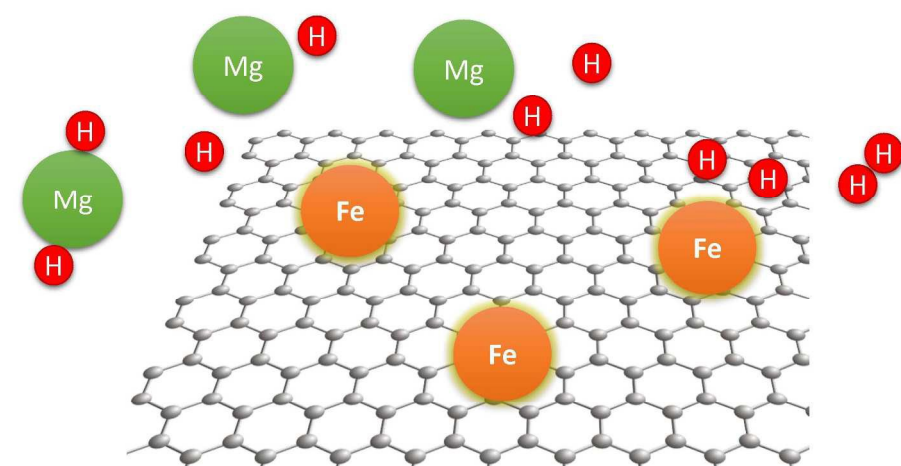
Acknowledgements

The authors acknowledge Hydrogen Energy Centre, Banaras Hindu University for providing the necessary experimental facilities. Financial support are from Department of Science and Technology (IFA12-PH-18) and Ministry of New and Renewable Energy (Mission Mode Project). Thanks to CMPDI, Ministry of Coal, India. One of the authors, Seema Awasthi acknowledges University Grants Commission for Financial support under the scheme, Dr DS Kothari PDF grant (No.F.4-2/2006(BSR)/13-768/2012(BSR)). CPU time is funded by Japan Society for the Promotion of Science. The calculation is performed at Hokkaido University academic cloud, information initiative center.

Notes and references

1. V. Georgakilas, M. Otyepka, A.B. Bourlinos, V. Chandra, N. Kim, K.C. Kemp, P. Hobza, R. Zboril and K.S. Kim, Functionalization of graphene: covalent and non-covalent approaches, derivatives and applications, *Chem. Rev.*, 2012, **112** (11), 6156-6214.
2. J. Pyun, Graphene Oxide as Catalyst: Application of Carbon Materials beyond Nanotechnology, *Angew. Chem. Int. Ed.*, 2011, **50** (1), 46-48.
3. C. Su, M. Acik, K. Takai, J. Lu, S.-j. Hao, Y. Zheng, P. Wu, Q. Bao, T. Enoki, Y.J. Chabal and K. P. Loh, Probing the catalytic activity of porous graphene oxide and the origin of this behavior, *Nat. Comm.*, 2012, **3**, 1298.
4. Y.H. Lu, M. Zhou, C. Zhang and Y.P. Feng, Metal-Embedded Graphene: A Possible Catalyst with High Activity, *J. of Phys. Chem. C*, 2009, **113**, 20156-20160.
5. H.R. Byon, J. Suntivich and Y. Shao-Horn, Graphene-based non-noble-metal catalysts for oxygen reduction reaction in acid, *Chem. of Mat.* 2011, **23** (15), 3421-3428.
6. S. Sabater, J.A. Mata and E. Peris, Catalyst Enhancement and Recyclability by Immobilization of Metal Complexes onto

- Graphene Surface by Noncovalent Interactions, *ACS Catal.*, 2014, **4** (6), 2038-2047.
7. K. Takahashi, Y. Wang, S. Chiba, Y. Nakagawa, S. Isobe and S. Ohnuki, Low temperature hydrogenation of iron nanoparticles on graphene, *Nat. Sci. Reports*, 2014, **4**, 4598.
 8. M.S.L. Hudson, H. Raghubanshi, S. Awasthi, T. Sadhasivam, A. Bhatnager, S. Simizu, S.G. Sankar, and O.N. Srivastava, Hydrogen uptake of reduced graphene oxide and graphene sheets decorated with Fe nanoclusters, *Int. J of Hydrogen Energy*, 2014, **39** (16), 8311-8320.
 9. K. Takahashi, S. Isobe, and S. Ohnuki, H₂ dissociation over NbO: The first step toward hydrogenation of Mg, *Langmuir* 2013, **29** (38), 12059-12065.
 10. K. Takahashi, S. Isobe and S. Ohnuki, The catalytic effect of Nb, NbO and Nb₂O₅ with different surface planes on dehydrogenation in MgH₂: Density functional theory study, *J. of Alloys and Comp.*, 2013, **580**, S25-S28.
 11. G. Barkhordarian, T. Klassen and R. Bormann, Fast hydrogen sorption kinetics of nanocrystalline Mg using Nb₂O₅ as catalyst, *Scripta Materialia*, 2003, **49** (3), 213-217.
 12. A. Anastasopol, T.V. Pfeiffer, J. Middelkoop, U. Lafont, R.J. Canales-Perez, A. Schmidt-Ott, F.M. Mulder and S.W. Eijt, Reduced enthalpy of metal hydride formation for Mg-Ti nanocomposites produced by spark discharge generation, *J. Am. Chem. Soc.*, 2013, **135** (21), 7891-7900.
 13. T. Sadhasivam, M.S.L. Hudson, S.K. Pandey, A. Bhatnagar, M.K. Singh, K. Gurunathan and O.N. Srivastava, Effects of nano size mischmetal and its oxide on improving the hydrogen sorption behaviour of MgH₂, *Int. J of Hydrogen Energy*, 2013, **38** (18), 7353-7362.
 14. S.K. Pandey, A. Bhatnagar, R.R. Shahi, M.S.L. Hudson, M.K. Singh and O.N. Srivastava, Effect of TiO₂ Nanoparticles on the Hydrogen Sorption Characteristics of Magnesium Hydride, *J. Nanosci. and Nanotech.*, 2013, **13**, 5493-5499.
 15. H.E. Kissinger, Reaction Kinetics in Differential Thermal Analysis, *Anal. Chem.* 1957, **29** (11), 1702-1706.
 16. M. Pourabdoli, S. Raygan, H. Abdizadeh and D. Uner, Determination of kinetic parameters and hydrogen desorption characteristics of MgH₂ 10 wt% (9Ni 2Mg Y) nano composite, *Int. J of Hydrogen Energy* 2013, **38** (27), 11910-11919.
 17. L. Zhang, L. Chen, X. Xiao, X. Fan, J. Shao, S. Li, H. Ge and Q. Wang, Fluorographene nanosheets enhanced hydrogen absorption and desorption performances of magnesium hydride, *Int. J of Hydrogen Energy* 2014, **39** (24), 12715-12726.
 18. G. Liu, Y. Wang, C. Xu, F. Qiu, C. An, L. Li, L. Jiao and H. Yuan, Excellent Catalytic Effects of Highly Crumpled Graphene Nanosheets on Hydrogenation/Dehydrogenation of Magnesium Hydride, *Nanoscale* 2013, **5**, 1074-1081.
 19. M. Paskevicius, D.A. Sheppard and C.E. Buckley, Thermodynamic Changes in Mechanochemically Synthesized Magnesium Hydride Nanoparticles, *J. Am. Chem. Soc.* 2010, **132** (14), 5077-5083.
 20. W. Liu, E.J. Setijadi and K.F. Aguey Zinsou, Tuning the Thermodynamic Properties of MgH₂ at the Nanoscale via a Catalyst or Destabilizing Element Coating Strategy, *J. Phys. Chem. C* 2014, **118** (48), 27781-27792.
 21. Z. Zhao Karger, J. Hu, A. Roth, D. Wang, C. Kübel, W. Lohstroh and M. Fichtner, Altered thermodynamic and kinetic properties of MgH₂ infiltrated in microporous scaffolds, *Chem. Comm.* 2010, **46**, 8353-8355.
 22. Y. Jia, C.H. Sun, N. Cheng, M.A. Wahab, J. Cui, J. Zou and X. Yao, Destabilization of Mg-H bonding through nano-interfacial confinement by unsaturated carbon for hydrogen desorption from MgH₂, *Phys. Chem. Chem. Phys.* 2013, **15**, 5814-5820.
 23. M. Ismail, N. Juahir and N.S. Mustafa, Improved Hydrogen Storage Properties of MgH₂ Co Doped with FeCl₃ and Carbon Nanotubes, *J. Phys. Chem. C* 2014, **118** (33), 18878-18883.
 24. G. Liu, Y. Wang, L. Jiao, and H. Yuan, Understanding the Role of Few Layer Graphene Nanosheets in Enhancing the Hydrogen Sorption Kinetics of Magnesium Hydride, *ACS Appl. Mater. Interfaces* 2014, **6** (14), 11038-11046.
 25. S. Pevzner, I. Pri Bar, I. Lutzky, E. Ben Yehuda, E. Ruse and O. Regev, Carbon Allotropes Accelerate Hydrogenation via Spillover Mechanism, *J. Phys. Chem. C* 2014, **118** (46), 27164-27169.
 26. Y. Lin, F. Ding and B.I. Yakobson, Hydrogen storage by spillover on graphene as a phase nucleation process, *Phys. Rev. B* 2008, **78**, 041402 (R).
 27. A.L. Patterson, The Scherrer Formula for X Ray Particle Size Determination, *Phys. Rev.* 1939, **56**, 978.
 28. M. Danaie, A.C. Asselli, J. Huot and G.A. Botton, Formation of the Ternary Complex Hydride Mg₂FeH₆ from Magnesium Hydride (β MgH₂) and Iron: An Electron Microscopy and Energy Loss Spectroscopy Study, *J. Phys. Chem. C* 2012, **116** (49), 25701-25714.
 29. J.J. Mortensen, L.B. Hansen and K.W. Jacobsen, Real space grid implementation of the projector augmented wave method, *Phys. Rev. B* 2005, **71**, 035109.
 30. J.P. Perdew, K. Burke and M. Ernzerhof, Generalized gradient approximation made simple, *Phys. Rev. Lett.* 1996, **77**, 3865.
 31. E. Sanville, S.D. Kenny, R. Smith and G. Henkelman, Improved grid based algorithm for Bader charge allocation, *J. of Comp. Chem.* 2007, **28**, 899-908.
 32. G. Henkelman, A. Arnaldsson and H.A. Jónsson, A fast and robust algorithm for Bader decomposition of charge density, *Com. Mat. Sci.* 2006, **36** (3), 354-360.



208x190mm (300 x 300 DPI)